

The Airway-Epithelium: A Novel Site of Action by Guanylin

Zhi Hao Zhang, Flora Jow, Randal Numann, and Joseph Hinson

Division of CNS, Wyeth-Ayerst Research, CN 8000, Princeton, New Jersey 08543

Received January 8, 1998

We studied the activation of a chloride channel in normal human bronchial epithelial cells (NHBE) by guanylin. We have observed a background Cl current ($I_{Cl,background}$) and a guanylin-induced outward rectifying chloride currents (ORCC) in NHBE. $I_{Cl,background}$ was present in 93% of cells ($n=114$), was outwardly-rectifying, and could be completely blocked by $100\mu M$ NPPB (5-Nitro-2(3-phenyl-propylamino)-benzoic acid. Activation of cAMP-activated Cl current with $200\mu M$ CPT-cAMP (8-(4-Chlorophenylthio) adenosine-3',5'-monophosphate) occurred in only 35.3% of cells ($n=34$). Guanylin activated an ORCC in 78.6% ($n=11$) of cells. Guanylin also induced chloride currents in cells that had failed to respond to CPT-cAMP ($n=5$). Both CPT-cAMP and the guanylin-induced chloride currents showed strong outward rectification. $500\mu M$ DIDS (4,4'-diisothiocyanostibene-2,2'-disulfonic acid) blocked the guanylin-induced ORCC ($n=10$). Conclusion: Guanylin activates a DIDS-sensitive ORCC in the NHBE cell which is only modestly activated by cAMP. The guanylin receptor in the NHBE might be of major importance in the regulation of chloride channel activity and transepithelial fluid transport in normal and abnormal airways. © 1998 Academic Press

The association of cystic fibrosis with low-chloride conductance of airway epithelia has led to extensive efforts to elucidate alternate pathways for chloride channel activation in the airways. In cystic fibrosis the CFTR (Cystic Fibrosis Transmembrane Regulator) chloride channel is genetically-rendered defective. Transepithelial electrolyte transport in the airway epithelium becomes inadequate resulting in impaired pulmonary mucociliary clearance and ultimately respiratory failure. Thus much research in the past had focused on the CFTR channel and signaling pathways that lead to its activation. It is now well established that CFTR activity requires phosphorylation by a cAMP-dependent protein kinase (PKA). However more

recent reports seem to indicate that other regulatory pathways for CFTR might exist (1-3).

Of particular interest to us was the potential role of a cGMP-mediated pathway. This is a major mechanism in intestinal epithelia for CFTR activation. The endogenous stimulator of the intestinal cGMP-mediated pathway has been identified as guanylin, a 15-amino acid peptide that possesses structural homology with heat-stable bacterial enterotoxin (STa) which is responsible for secretory diarrhoea (4). Both STa and guanylin have been shown to elevate cGMP levels and concomitantly activate CFTR in intestinal epithelial cells (5). To investigate whether a similar cGMP pathway might exist in the airway epithelium, we considered utilizing guanylin based on some very recent findings: guanylin is secreted into the airways by Clara cells of the lungs (6), STa receptors can be found in tracheal epithelia (7), and membrane-bound guanylate cyclases (A, B, and C) exist in the airway epithelia and cGMP elevations can be elicited with the natriuretic peptides and STa (8). In this report, we demonstrate that guanylin potentially stimulates airway epithelial chloride currents.

MATERIALS AND METHODS

Cell culture. Normal human bronchial epithelial cells (NHBE) were purchased from Clonetics Corporation (San Diego, CA). NHBE cells were isolated from human tracheobronchial epithelium collected at the time of autopsy. Cells were delivered by Clonetics cryopreserved at passage 2 and cultured in our laboratory in bronchial epithelial cell growth medium (BEGM) which is a modified LHC-9 formulation containing the following supplements essential for cell differentiation and proliferation: bovine pituitary extract, hydrocortisone, human epidermal growth factor, epinephrine, transferrin, insulin, retinoic acid, triiodothyronine, gentamycin and amphotericin B(9). Cells were maintained in culture at 37 °C in 5% CO₂/95% humidified air for 3 to 5 days before use. All experiments were conducted on cells in passage 3 or 4.

Solutions and drugs. The normal external solution contained (in mM): NaCl 140, MgCl₂ 2, CaCl₂ 2 and 4-(2-hydroxyethyl)-1-piperazine ethanesulfonic acid (HEPES) 10. The normal pipette solution contained (in mM): KCl 125, HEPES 10, MgCl₂ 2, ethylenedis(oxonitrilo)tetraacetate (EGTA) 2, and ATP_{Mg} 5. For isolating chloride cur-

rents, Na^+ and K^+ were replaced by NMDG and the pH was adjusted to 7.3 with methanesulfonic acid or Tris. To separate the leak conductance from chloride currents, internal Cl^- ion concentration was reduced to 45 mM using glutamic acid ($E_{\text{rev}(\text{Cl})}$ approximately -31 mV from the Nernst equation).

NPPB was obtained from Calbiochem (La Jolla, CA). Guanylin was purchased from Peninsula Laboratories, Inc. (Belmont, CA). All other drugs were from Sigma Chemicals unless indicated otherwise.

Voltage-clamp recording. The whole cell patch clamp recording technique was used to record membrane ionic currents (10, 11). Prior to recording from them, NHBE cells were partially detached using trypsin and then perfused with normal external solution. This produced a more rounded profile for the cells which facilitated patch recording and cell isolation. Voltage clamp experiments were performed on nonconfluent single cells at room temperature. The volume of the external solution in the recording chamber (35mm culture dish) was approximately 2 ml and the rate of perfusion was 6 ml/min. Membrane currents were recorded using an Axopatch 200A Patch Clamp Amplifier (Axon Instruments, Inc., Foster City, CA). After obtaining a giga ohm-seal ($45.2 \pm 8.2 \text{ G}\Omega$, $n = 114$), additional suction was applied to break the cell membrane and enter the whole-cell configuration. Capacitive currents elicited by a 10 mV depolarizing pulse from -80 mV were recorded and then compensated. Representative capacitive traces were used to calculate cell capacitance determined using the equation $C_m = \tau_c \cdot I_0 / \Delta E_m$ (11), where C_m = membrane capacitance, τ_c is the time constant for cell membrane charge, I_0 is the peak of the capacitive current and ΔE_m is clamp potential. The C_m varied from 7.8 to 162 pF with an average of $47.4 \pm 3.1 \text{ pF}$ ($n = 114$). Membrane currents were generated by the following three voltage pulse protocols: 1) For drug-effect time course experiments; V_h (holding potential) = -30 mV, V_c (clamp potential) = 60 mV and T_c (clamp time) = 1 s. 2) For voltage ramp experiments; $V_h = -30 \text{ mV}$, V_{ramp} (ramp potential range) = -100 to 100 mV, $T_{\text{ramp}} = 3 \text{ s}$. 3) For current-voltage step experiments (I-V); $V_h = -30 \text{ mV}$, $V_c = -120$ to 120 mV with 20 mV (or 10 mV) steps and $T_c = 1 \text{ s}$. In all three protocols the voltage pulses or ramps were applied at 0.1 Hz.

Data analyses. Membrane currents were digitally recorded and analyzed using pCLAMP software (pCLAMP Version 6.0.1, Axon Instruments Inc., Foster City, CA). Further analyses of data and preparation of figures were accomplished with the program suite, Microsoft Excel and ORIGIN (MicroCal, Northampton, MA.). Data were presented as Mean \pm SEM. Student's t-test for paired data was used to compare control conditions with other interventions. A p value of < 0.05 was considered statistically significant.

RESULTS

The characteristics of the background chloride current, $I_{\text{Cl,background}}$. The human bronchial epithelial cell cultures (NHBE) contained a background chloride current as previously reported by us (12). In order to fully differentiate the effects of guanylin, we first characterized this background current in solutions where the sodium and potassium were replaced by NMDG (methods). The background chloride current, $I_{\text{Cl,background}}$, was observed in the majority of cells (93 % of cells; 106 out of 114) and were $2.7 \pm 0.5 \text{ pA/pF}$ at 60 mV. Any cell with a current of less than 50 pA at 100 mV was considered devoid of a significant background current. $I_{\text{Cl,background}}$ exhibited strong outward rectification, but the degree of rectification varied from cell to cell. The $I_{\text{Cl,background}}$ current was seen to run down over time.

Run-down started immediately after cell-membrane break-in but slowed greatly after 8 min in 6 of 10 cells. The averaged run-down was $43 \pm 5.3 \%$ (from 5.3 ± 1.7 to $2.8 \pm 0.8 \text{ pA/pF}$ at 60 mV, $n = 6$). In general the kinetics for $I_{\text{Cl,background}}$ were fast activating ($< 2 \text{ ms}$) and sustained although in 19 out of 106 cells an inactivating phase could be seen at voltage above 60 mV and in 7 out of 106 cells slow activating kinetics were observed. The time constant of inactivation and activation at 100 mV was $1291 \pm 417 \text{ ms}$ ($n = 19$) and $442 \pm 79 \text{ ms}$ ($n = 6$) respectively. The inactivation and activation became progressively faster as the potential was clamped to more positive potentials.

To ascertain whether the background current was predominantly carried by chloride ions, the cells were exposed to three different external solutions ($[\text{Cl}]_o$), containing chloride concentrations of 148, 95 and 15 mM, while $[\text{Cl}]_{\text{in}}$ of pipette solution was kept at 45 mM. The results showed that the values of the reversal potential for chloride, $E_{\text{rev}(\text{Cl})}$, were -26.7 ± 2.2 , -13.6 ± 2.4 and $20 \pm 2.2 \text{ mV}$ at $[\text{Cl}]_o$ of 148, 95 and 15 mM respectively ($n = 7$). The $E_{\text{rev}(\text{Cl})}$ of chloride were plotted against the $\log [\text{Cl}]_o$ and was fitted by a linear equation ($y = a + k \cdot X$) expressed as a solid line going through the data points (Figure not shown). The slope k , representing the changes in $E_{\text{rev}(\text{Cl})}$ with a 10-fold $[\text{Cl}]_o$ increment, was 45.5 mV/decade. This result is close to the theoretical value for a pure Cl^- selective channel (55.3 mV/decade), which shows that the background Cl^- current is largely Cl^- selective.

The CPT-cAMP-induced chloride current. Since guanylin could be influencing the cAMP activation pathway, we found it appropriate to evaluate the characteristics of a cAMP-induced chloride current in our preparation. An outwardly-rectifying time-independent current was induced at room temperature in the presence of 200 μM CPT-cAMP (CPT) in 35.3 % of cells (12 out of 34) examined. In responding cells 200 μM CPT-cAMP increased the chloride current 11 ± 3.1 fold from 5.5 ± 1.4 to $52.1 \pm 20.2 \text{ pA/pF}$ ($n = 12$, $p < 0.01$). The CPT-cAMP-induced chloride current was partially reversed ($29.1 \pm 12.8 \%$) upon washout ($n = 4$) and fully blocked by 0.1 mM NPPB ($96.4 \pm 0.06 \%$, $n = 2$). An example of these experiments is illustrated in Figure 1A. The three top panels show the steady state control current, the CPT-cAMP-induced current and the ramp currents recorded before and after application of CPT-cAMP. It is evident from voltage step data and the ramp that the CPT-cAMP-induced current is time-independent and outwardly rectified. The inset of figure 1A displays the averaged ramp current from 12 experiments and shows strong outward rectification of the CPT-induced chloride current. The bottom panel of figure 1A shows the time course from a single experiment at a test voltage of 60 mV. The effect of CPT

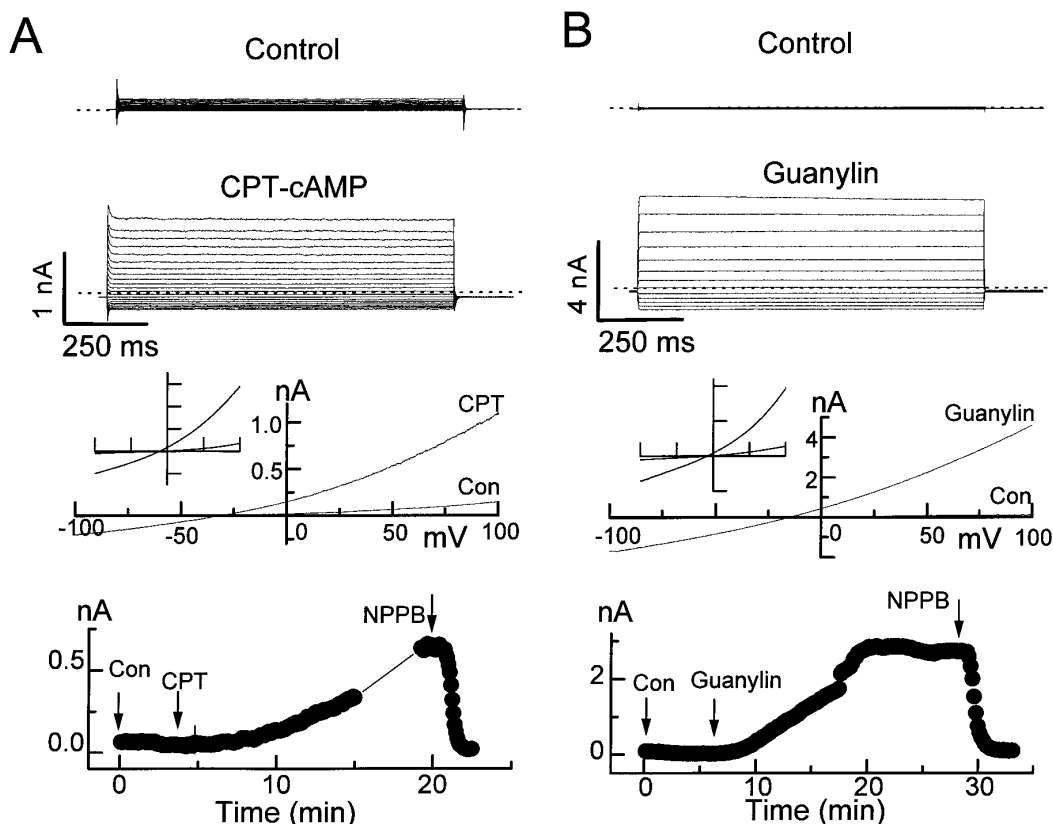


FIG. 1. Characterization of the chloride channel induced by CPT-cAMP and guanylin. In panel A, the top two traces are control and after 18 min of CPT-cAMP perfusion. The dotted line indicate 0 pA. The 3rd panel from the top is the ramp I-V recorded in the presence (CPT) and absence (C) of CPT-cAMP solution. The inset is averaged normalized ramp currents before and during CPT-cAMP ($n=12$). In the bottom panel of figure A, the amplitude of the ORCC was measured at 60 mV and plotted against time for the same cell shown in panel 3. The ORCC was induced by 200 μ M CPT-cAMP and fully blocked by NPPB 0.1 mM. Panel B: Identical experiments were carried out to with guanylin activation of the chloride current. The top two panels show recording in control solution and after application of guanylin 1 μ M for 15 min. The dotted line indicates 0 pA. The 3rd panel from the top is the ramp I-V recorded in the presence and absence guanylin. The inset is the averaged ramp current from 10 cells before and during guanylin. The bottom panel is the time course of an experiment from the same cell as in panel 3 illustrating the activation of ORCC by 1 μ M guanylin and block by NPPB 100 μ M.

reached a steady state within 15 min and the current was completely inhibited within 2 min by application of 0.1 mM NPPB.

The guanylin-induced chloride current. We tested the effect of guanylin on NHBE cell and compared its activity with that of CPT-cAMP. A time-independent current was induced at room temperature in the presence of 1-5 μ M guanylin. 78.6 % of cells (11 out of 14) showed significant responses within 5-10 min of guanylin application. Thus, compared to a maximal concentration of CPT-cAMP which induced currents only 35.3 % of the time, guanylin had a much higher rate for the activation of chloride currents in airway epithelial cells, despite the relatively low concentration of peptide applied. The results show that the chloride current was increased to 41.7 pA/pF from 2.3 ± 0.6 pA/pF in the presence of guanylin (32.7 ± 17.7 times, $n = 11$). Guanylin-induced chloride currents were not reversible after 5-10 min of washout (only reduced by 15.8 ± 11.3

%, $n = 2$) but were fully blocked by 0.1 mM NPPB (96.5 ± 0.84 %, $n = 4$). An example of the experiments is illustrated in figure 1B. The three top panels of figure 1B show the steady state control current, 1 μ M guanylin-induced current and the ramp currents before and after application of guanylin. The inset shows averaged ramp currents from 11 cells. The bottom panel of figure 1B shows the time course of the experiment at a test voltage of 60 mV from the same cell. The effect of guanylin reached a steady state within 15 min and the current was completely inhibited in 2 min by 100 μ M NPPB. The results indicate that guanylin has a much higher activity than CPT-cAMP on the chloride channel but the time to reach the maximum effect is slower compared to CPT-cAMP.

Because guanylin appears to activate chloride channels more effectively than CPT-cAMP, we conducted further experiments to see if guanylin could stimulate the chloride channel in cells that were partially or com-

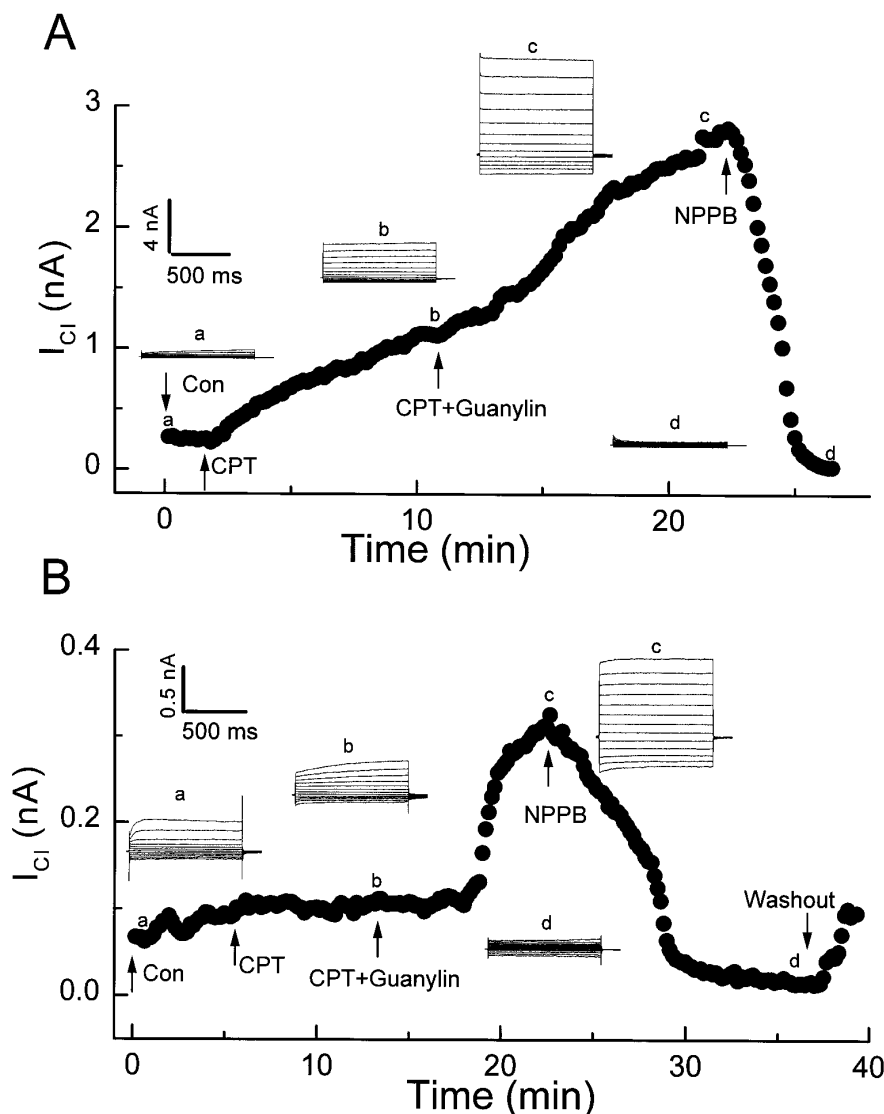


FIG. 2. Outward rectifying chloride channel (ORCC) activity activated by 200 μ M CPT-cAMP (CPT) and 1 μ M guanylin from same cell. Panel A: The amplitudes measured at 60 mV were plotted against the time for control and after application of CPT and guanylin. The figure shows that CPT partially activates a ORCC after 10 min, at which time 1 μ M guanylin is applied which dramatically increases the rate of activation of ORCC. 100mM NPPB completely blocks the current. The current traces indicated by (a), (b), (c) and (d) were recorded from control, CPT, CPT + guanylin and NPPB. Figure B shows that a 10 minute application of CPT-cAMP fails to activate ORCC in this cell, however ORCC was dramatically increased by subsequent addition of 1 μ M guanylin. This guanylin sensitive current was fully blocked by NPPB 100 μ M. The traces indicated by (a), (b), (c) and (d) were recorded from control, CPT, CPT + guanylin and NPPB, respectively.

pletely unresponsive to CPT-cAMP. The experiments show that guanylin not only further increased the chloride currents partially activated by CPT-cAMP ($n = 2$), but also activate the currents in cells that did not respond to CPT-cAMP ($n = 2$). The averaged data from five cells show that CPT-cAMP partially activate the current from 4 ± 1.1 to 10.8 ± 3.7 pA/pF (3.2 ± 0.8 times, $n = 5$, $p > 0.05$) and that guanylin further increase the amplitude of this current to 27.8 ± 7.9 pA/pF (2.8 ± 0.3 times, $n = 5$, $p < 0.05$). NPPB at 100 μ M completely blocked all chloride currents including the

background, CPT-cAMP- and guanylin- induced currents. The magnitude of current enhancement by guanylin was slightly lower in these CPT-cAMP-insensitive cells (27.8 ± 7.9 vs. 41.7 ± 17.5 pA/pF). Figure 2A is an example of these experiments. The inset shows the current traces recorded from control (a), in the presence of CPT-cAMP (b), guanylin (c), and NPPB (d). Figure 2B shows an outward rectifying chloride current activated by 1 μ M guanylin but not by 200 μ M CPT-cAMP. The inset shows current traces recorded from control (a), in the presence of CPT-cAMP (b), guanylin (c), and

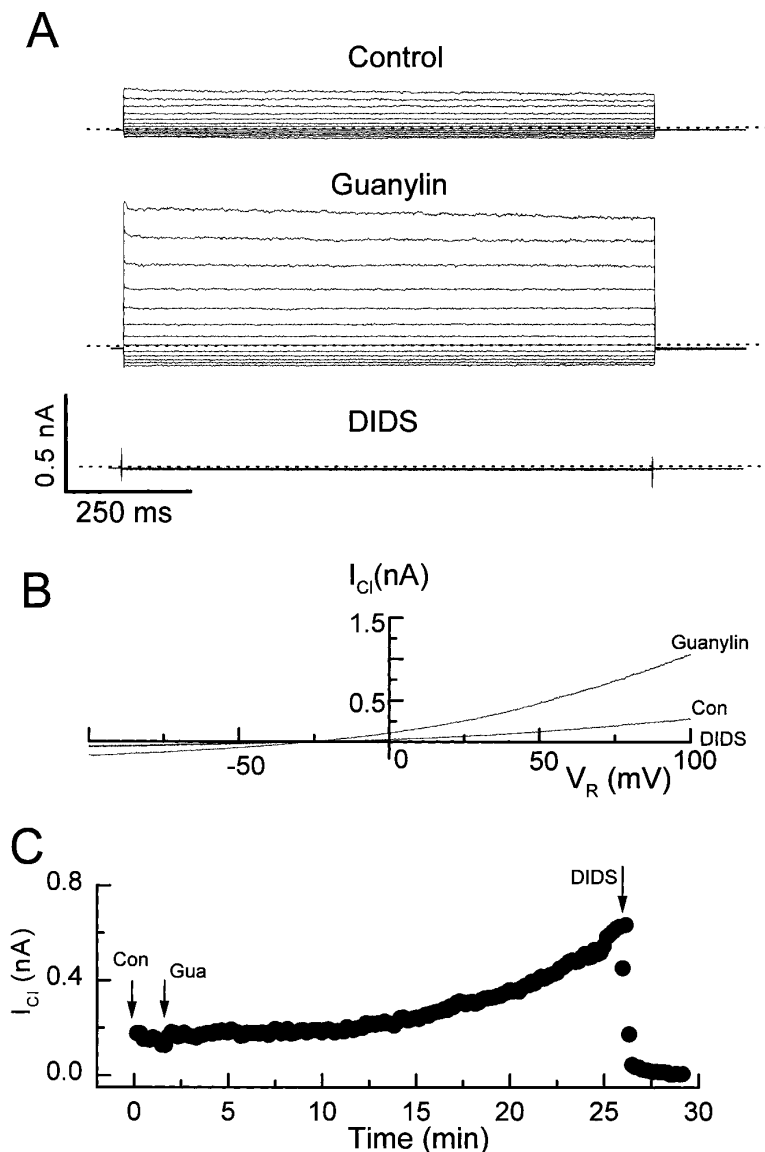


FIG. 3. Panel A illustrate the background, guanylin-induced current and a residual current after application DIDS 0.5 mM. The dot line indicate the base line. In panel B, a ramp currents are shown for control, guanylin and DIDS. Panel C shows the time course of the experiment during control, 20 min of guanylin application and 5 min of DIDS exposure for test pulse to 60 mV.

NPPB (d). The above results suggest that guanylin has a greater ability to induce chloride channels in airway epithelial cells than does CPT-cAMP.

The effects of other cyclic-nucleotide mobilizing peptides. In order to ensure that the effects by guanylin were not due to non-specific peptidergic effects, we also evaluated other peptides, pituitary adenyl cyclase activating peptide (PACAP38), secretin, and adrenomedullin on these airway cells to ascertain if they also induced chloride currents. These peptides have been reported to mobilize cAMP in various tissues (13-18). In fourteen experiments, PACAP38 ($n = 7$), Secretin ($n =$

3) and Adrenomedullin ($n = 4$) had no significant effect on the airway chloride currents. Therefore we concluded that unlike guanylin, these peptides fail to induce chloride currents in the airway epithelial cell.

Sensitivity of chloride currents to DIDS. It has been reported that in airway epithelia, outward rectifying chloride currents (ORCC) is much more sensitive to DIDS, compared to CFTR (19). Thus we used DIDS to help determine whether the guanylin-induced chloride current was likely to be ORCC or CFTR. 14 cells were tested after induction of chloride currents in the presence of 1-5 μ M guanylin. An outwardly-rectifying chlo-

ride current was induced in 10 of 14 cells by guanylin after which 500 μM DIDS was added to the external solution for 10–20 min. Ten experiments showed that DIDS (0.5 mM) strongly blocked the guanylin-induced current from 11.4 ± 3.3 to $0.49 \pm .29$ pA/pF at 60 mV ($n = 10$, $p < 0.01$). An example of these experiments is depicted in figure 3. Guanylin (5 μM) activate a large outwardly rectifying chloride current that is completely blocked by 500 μM DIDS as is the background chloride current seen in control. Similar results were obtained from the ramp currents recorded in the presence of control, guanylin-containing, and DIDS-containing solutions, as depicted in figure 3B. The time course of current changes in the presence of guanylin and DIDS at 60 mV are illustrated in figure 3C. Chloride current increase 5 fold within 20 min of guanylin application, and this guanylin-induced current is completely blocked by DIDS (500 μM).

DISCUSSION

The data presented suggest that (a) human airway epithelial cells possess a small background chloride conductance. (b) Guanylin activates an outwardly-rectifying, chloride current that is blocked by 500 μM DIDS. (c) The action by guanylin seems to be quite specific since other cyclic nucleotide-mobilizing peptides such as adrenomedullin, secretin, and PACAP-38, have no effect on the airway epithelial chloride currents. (d) There is no evidence for a DIDS-insensitive CFTR current activated by guanylin in this airway cell culture.

It is of interest that guanylin activates a predominantly outward-rectifying chloride current in the present study. Most reports have demonstrated a guanylin-cGMP-dependent activation of CFTR currents with a linear current-voltage relationship (20). Furthermore, in the present study, the guanylin-induced currents could be blocked by 500 μM DIDS, which according to most reports, does not block the CFTR chloride channel (19).

The fact that the observed currents were outwardly-rectifying and blocked by 500 μM DIDS could be the result of a secondary activation of ORCC by a guanylin-stimulated CFTR. This link between the two chloride channels has recently been demonstrated by other investigators (19). In fact, in this study CPT-cAMP also activated outwardly-rectifying currents. On the other hand, guanylin could be exerting a direct action on ORCC. The guanylin receptor, Guanylate Cyclase type C (GCC) has a protein tyrosine kinase activity in addition to its better-known guanylate cyclase activity (21) but the ion-channel target of the tyrosine kinase has not yet been identified. Thus, guanylin's action on epithelial chloride channels is not limited to the gastrointestinal tract and the peptide can elicit effects on the

airway as well. This finding seems to be consistent with the accumulating evidence that guanylin might also be associated with the airways. Using immunoblot analyses and immunocytochemistry, investigators have determined that Clara cells of the lungs are a major source of guanylin in the airways (6). Furthermore, guanylate cyclase C, the putative guanylin receptor, has been found to be expressed in human and bovine airway epithelia (22). In vitro receptor autoradiography has revealed the presence of STa-binding receptors in airway epithelia of the opossum (7). The bacterial heat-stable enterotoxin STa has structural homology with guanylin and act on the same receptor. The stimulation by cGMP of airway epithelial chloride channel has also recently been reported (23).

Single-channel recording would be necessary to help establish the true identity of the chloride channel activated by guanylin. It also remains to be demonstrated if inhibitors of protein tyrosine kinase can block the activation of ORCC by guanylin. Further experiments would also be appropriate in determining if guanylin can activate chloride currents in airway epithelia in the presence of protein kinase A inhibitors, or with an antibody against CFTR. In conclusion this study shows that guanylin is a potent activator of an ORCC in primary cultured human airway epithelial cells and that guanylin can activate this current in cells which are unresponsive to CPT-cAMP. This suggests that guanylin is directly activating ORCC in these airway cells.

REFERENCES

1. Illek, B., Fischer, H., and Machen, T. E. (1996) *Am. J. Physiol.* **270**, C265–C275.
2. Shintani, Y., and Marunaka, Y. (1996) *Biochem. Biophys. Res. Commun.* **223**, 234–239.
3. Dong, Y.-J., Chao, A. C., Kuoyama, K., Hsu, Y.-P., Bocian, R. C., Moss, R. B., and Gardner, P. (1995) *EMBO J.* **14**, 2700–2707.
4. Currie, M. G., Fok, K. F., Kato, J., Moore, R. J., Hamra, F. K., Duffin, K. L., and Smith, C. E. (1992) *Proc. Natl. Acad. Sci. USA* **89**, 947–951.
5. Chao, A., de Sauvage, F. J., Dong, Y.-J., Wagner, J. A., Goeddel, D. V., and Gardner, P. (1994) *EMBO J.* **13**, 1065–1072.
6. Cetin, Y., Kulaksiz, H., Redecker, P., Bargsten, G., Adermann, K., Grube, D., and Forssmann, W.-G. (1995) *Proc. Natl. Acad. Sci. USA* **92**, 5925–5929.
7. Krause, W. J., Freeman, R. H., and Forte, L. R. (1990) *Cell Tissue Res.* **260**, 387–394.
8. Range, S. P., Holland, E. D., Basten, G. P., and Knox, A. J. (1997) *Br. J. Pharmacol.* **120**, 1249–1254.
9. Gruenert, D. C., Finkbeiner, W. E., and Widdicombe, J. H. (1995) *Am. J. Physiol.* **268**, L347–L360.
10. Chan, H.-C., Golstein, J., and Nelson, D. J. (1992) *Am. J. Physiol.* **262**, C1273–C1283.
11. Zhang, Z. H., and Steinberg, M. I. (1995) *J. Pharmacol. Exp. Ther.* **274**, 249–257.
12. Zhang, Z. H., Jow, F., Hinson, J., Numann, R., and Colatsky, T. J. (1997) *Biophys. J.* **72**, 412.

13. Kuwahara, A., Kuwahara, Y., Mochizuki, T., and Yanaihara, N. (1993) *Am. J. Physiol.* **264**, 433–G441.
14. Salomon, R., Couvineau, A., Rouyer, F. C., Voisin, T., Lavallee, D., Blais, A., Darmoul, D., and Laburthe, M. (1993) *Am. J. Physiol.* **264**, E294–E300.
15. Rolston, D. D. K., Rolston, R. K., Shin, K., Blochin, B., Cabungal, C., Anbar, R., Holsclaw, D. S., Kreuger, L. J., and Lebenthal, E. (1993) *Pediatric Res.* **33**, 385a.
16. McGill, J. M., Basavappa, S., Gettys, T. W., and Fitz, J. G. (1994) *Am. J. Physiol.* **266**, G731–G736.
17. Martinez, A., Miller, M. J., Catt, K. J., and Cuttitta, F. (1997) *J. Histochem. Cytochem.* **45**, 159–164.
18. Shimekake, Y., Nagata, K., Ohta, S., Kambayashi, Y., Teraoka, H., Kitamura, K., Eto, T., Kangawa, K., and Matsuo, H. (1995) *J. Biol. Chem.* **270**, 4412–4417.
19. Schwiebert, E. M., Egan, M. E., Hwang, T-H., Fulmer, S. B., Allen, S. S., Cutting, G. R., and Guggino, W. B. (1995) *Cell* **81**, 1063–1073.
20. Cliff, W. H., and Frizzel, R. A. (1990) *Proc. Natl. Acad. Sci. USA* **87**, 4956–4960.
21. Drewett, J. G., and Garbers, D. L. (1994) *Endocr. Rev.* **15**, 135–161.
22. Schulz, S., Christian, T. D., and Garbers, D. L. (1992) *J. Biol. Chem.* **267**, 16019–16021.
23. Schwiebert, E. M., Potter, E. D., Hwang, T. H., Woo, J. S., Ding, C., Qiu, W., Guggino, W. B., Levine, M. A., and Guggino, S. E. (1997) *Am. J. Physiol.* **272**, C911–C922.